Multiobjective System Sizing for Heavy-Duty Electric Vehicle Charging Stations

Ashkezari, Leila Shams; Mouli, Gautham Ram Chandra; Yorke-Smith, Neil; Bauer, Pavol

DOI
10.1109/ESARS-ITEC60450.2024.10819791

Publication date
2024

Document Version
Final published version

Published in
2024 IEEE International Conference on Electrical Systems for Aircraft, Railway, Ship Propulsion and Road Vehicles and International Transportation Electrification Conference, ESARS-ITEC 2024

Citation (APA)
Ashkezari, L. S., Mouli, G. R. C., Yorke-Smith, N., & Bauer, P. (2024). Multiobjective System Sizing for Heavy-Duty Electric Vehicle Charging Stations. In *2024 IEEE International Conference on Electrical Systems for Aircraft, Railway, Ship Propulsion and Road Vehicles and International Transportation Electrification Conference, ESARS-ITEC 2024* (2024 IEEE International Conference on Electrical Systems for Aircraft, Railway, Ship Propulsion and Road Vehicles and International Transportation Electrification Conference, ESARS-ITEC 2024). IEEE. https://doi.org/10.1109/ESARS-ITEC60450.2024.10819791

2024 IEEE International Conference on Electrical Systems for Aircraft, Railway, Ship Propulsion and Road Vehicles & International Transportation Electrification Conference (ESARS-ITEC) | 979-8-3503-7390-5/24/$31.00 ©2024 IEEE | DOI: 10.1109/ESARS-ITEC60450.2024.10819791

Multiobjective System Sizing for Heavy-Duty Electric Vehicle Charging Stations

Leila Shams Ashkezari
Dept. of Electrical Sustainable Energy
Delft University of Technology
Delft, Netherlands
l.shamsashkezari@tudelft.nl

Gautham Ram Chandra Mouli
Dept. of Electrical Sustainable Energy
Delft University of Technology
Delft, Netherlands
g.r.chandramouli@tudelft.nl

Neil Yorke-Smith
Dept. of Algorithmics
Delft University of Technology
Delft, Netherlands
n.yorke-smith@tudelft.nl

Pavol Bauer
Dept. of Electrical Sustainable Energy
Delft University of Technology
Delft, Netherlands
p.bauer@tudelft.nl

***Abstract*—The transportation industry is a significant source of greenhouse gas emissions, with freight transport emerging as one of the main contributors owing to its extensive mileage and substantial weight. As a result, electrification of road transportation has become a vital step in reducing direct CO_2 emissions. While the adoption of passenger electric vehicles has gained notable traction, the landscape for Heavy-Duty Electric Vehicles (HDEVs) is still in its early stages of development. Accelerating the advancement and adoption of HDEVs hinges on prioritizing the installation of their charging infrastructure. This requires a deep understanding of HDEVs' energy and power requirements while also considering grid limitations. Meeting the high demand for charging necessitates exploring on-site renewable energy generation and stationary batteries as viable solutions. Recognizing this imperative, a multiobjective sizing model has been developed, tailored specifically to address the requirements of HDEV charging stations. These objectives include minimizing investment costs, penalizing undercharged or rejected HDEVs' charging demand, reducing idle charger time, and managing expenditures within a charging station. The key outcomes of the model encompass various critical factors essential for designing and implementing charging infrastructure for HDEVs. These factors include determining the optimal number of PV panels and wind turbines to harness renewable energy, specifying the capacity of the battery energy storage system, and identifying the necessary number and rated power of chargers in alignment with the grid contract limit.**

***Index Terms*—Charging station configuration, Genetic algorithm (GA), Heavy-duty electric vehicle (HDEV), Multiobjective sizing model.**

I. Introduction

The European Commission took on a set of proposals to adapt the EU's climate, energy, mobility, and taxation practices in order to reduce net emissions by a minimum of 55% by 2030 and make this continent the first to achieve climate neutrality by 2050, which calls for a 90% reduction in emissions related to transportation by that year [3]. Road vehicles account for more than 75% of CO_2 emissions in the transportation sector according to [1] from which freight is responsible for over 30%, and it is likely to rise [2]. As a result, one of the most critical steps in reducing CO_2 emissions is the electrification of heavy-duty vehicles.

To promote the adoption of heavy-duty electric vehicles (HDEVs), the EU established a target of having HDEV-specific charging stations with a maximum distance of 60 km along the TEN-T core network by the end of 2030 to facilitate their excursions [4]. However, designing charging infrastructure for HDEVs comes with distinct challenges compared to passenger electric vehicles (EVs). Although, for now, battery size, charging demand, and energy consumption of HDEVs remain uncertain due to their limited availability and usage, HDEVs are expected to use notably large batteries ranging from 300 to 1000 kWh, leading to higher energy requirements. Furthermore, these trucks adhere to strict working schedules, constraining their charging availability and resulting in peak demand for charging. Consequently, charging stations for HDEVs must accommodate substantially higher charging rates—up to a few megawatts if multiple vehicles are charging simultaneously. Due to these challenges, existing models designed for passenger vehicles are unsuitable for sizing HDEV charging stations.

A significant amount of research has been dedicated to determining the appropriate sizes of distributed energy storage systems and renewable energy sources (RESs) for passenger EV charging station systems. However, there has been a noticeable scarcity of studies addressing the optimal number and power ratings of chargers required in a charging station. Moreover, the optimization objectives in many of these studies primarily focus on minimizing economic expenditure. Among the few papers that consider the sizing of chargers along with other factors, Bryden et al. [5] proposed a rule-based model for determining optimal battery energy storage system (BESS) capacity at passenger EV charging stations based on acceptable average waiting times, as well as determining the number of fast-charging connection points. However, their approach keeps the size of EV batteries, EV chargers' rated power, grid connection capacity, and acceptable waiting time of EVs constant. In [6], the optimal number of chargers and waiting spaces in fast charging stations was determined jointly to maximize expected operator profits, considering various factors such as charging service profit, waiting penalties, rejection penalties, and maintenance costs. However, their study, akin to [5], only optimizes the number of chargers while keeping their power constant, and they do not delve into sizing other assets such as RESs. Additionally, their rejection criteria for EVs are based solely on available space, neglecting considerations of parking times for vehicles. Dominguez-Navarro et al. [7] presented an approach utilizing a genetic algorithm (GA) model to optimize installation designs, including charger number, power ratings, wind turbine types, PV farm, and battery size. Their goal was to maximize profit measured by net present value (NPV). However, while their study seems to be more comprehensive in terms of variables optimized, they simplify the objectives by focusing only on economic considerations. While for a charging station such as those by highway, factors such as rejection and parking time penalties often hold more importance compared to economic variables. Hence, a noticeable research gap emerges where the sizing of BESS, RESs, and chargers are simultaneously considered, integrating additional objectives such as penalties related to unmet demand (rejection and undercharging of EVs) and idle chargers.

To address this gap, a bi-level multiobjective sizing model was developed to determine the size of assets in the charging station and identify the configuration. The optimization model seeks to find an HDEV charging station's configuration that balances multiple factors and objectives. These objectives include minimizing investment costs, penalizing undercharged or rejected HDEV charging demand, reducing idle charger time, and managing expenditures within a charging station. By considering these objectives collectively, the model aims to optimize various asset sizes within the charging station to maximize its economic and social benefits. The outcomes of this model are the number of PV panels and wind turbines, the capacity of BESS, the number of chargers, and their rated capacity according to the grid contract limit. In this model, if the defined grid limit proves insufficient to fulfill the minimum requirements within the system and a suitable configuration cannot be identified based on that, a dynamic adjustment mechanism is activated. This involves increasing the grid limit and restarting the model with the updated constraint so that the system can adapt effectively to minimum constraints and charging demands.

The subsequent sections of the paper are structured as follows: Section 2 outlines the methodology and constraints considered in defining the optimization model used for sizing assets. In Section 3, the input data and parameters of this model are detailed. Section 4 presents the conclusion of the study, showcasing the final results of the multiobjective model. Section 5 summarizes the paper and discusses future steps.

II. Mathematical Modelling

This study tries to identify the configuration and sizes of assets in an HDEV-specific charging station located along a highway in the Netherlands. To accomplish this, a bi-level multiobjective optimization model is defined. Given the anticipated charging demand, which is expected to reach several megawatts, and considering potential grid limitations and congestion, the inclusion of RESs and stationary BESS is deemed necessary for this charging station. The following section elaborates on the methodology and details of this sizing model.

In order to be able to define the multiobjective optimization model, NSGA-II (non-dominated sorting genetic algorithm II) is employed on this model [8]. NSGA-II enables the minimization of each objective independently, resulting in a range of non-dominated solutions at each generation. Moreover, NSGA-II offers the flexibility to prioritize objectives in the multiobjective optimization problem. By setting priorities for each objective and conducting a final selection process, different system configurations can be tailored to different limitations and objectives. For simplicity, the abbreviation GA is used instead of NSGA-II throughout this paper.

The optimization problem is subject to several hard constraints, equations (1)–(7), to ensure the correct performance of the system:

– limit of the SoC of the BESS (SoC^{min} as lower and SoC^{max} as upper bounds):

$$SoC^{\text{min}} \leq SoC_t^b \leq SoC^{\text{max}} \tag{1}$$

which leads to the limits of the charge ($P^{\text{bch, max}}$) and discharge power ($P^{\text{bdis, max}}$) of the BESS:

$$-P_t^{\text{bdis, max}} \leq P_t^{\text{b}} \leq P_t^{\text{bch, max}} \tag{2}$$

$$P_t^{\text{bch, max}} = \min(P^{\text{b, r}}, \frac{(SoC^{\text{max}} - SoC_t) \times E^{\text{b, r}}}{100 \times \Delta t}) \tag{3}$$

$$P_t^{\text{bdis, max}} = \min(P^{\text{b, r}}, \frac{(SoC_t - SoC^{\text{min}}) \times E^{\text{b, r}}}{100 \times \Delta t}) \tag{4}$$

– limit of the supplied and consumed power from the grid ($P^{\text{g, max}}$):

$$-P^{\text{g, max}} \leq P_t^{\text{g2s}} \leq P^{\text{g, max}} \tag{5}$$

– limit of the supplied power from the charger c to an HDEV ($P_{\text{t, c}}^{\text{s2ev}}$):

$$P_{\text{t, c}}^{\text{s2ev}} \leq P_{\text{c}}^{\text{r}} \tag{6}$$

– power balance in the charging station:

$$P_t^{\text{s2ev}} + P_t^{\text{s2g}} + P_t^{\text{unmet}} = P_t^{\text{pv}} + P_t^{\text{wind}} + P_t^{\text{b}} + P_t^{\text{g2s}} \tag{7}$$

where:

$$P_t^{\text{s2ev}} = \sum_{v=1}^{N^{ev}} P_{\text{t,v}}^{\text{ev}} \tag{8}$$

$$P_{\text{t}}^{\text{total}} = P_{\text{t}}^{\text{s2ev}} - P_{\text{t}}^{\text{b}} - P_{\text{t}}^{\text{pv}} - P_{\text{t}}^{\text{wind}} \tag{9}$$

$$P_{\text{t}}^{\text{g2s}} = \begin{cases} \min(P^{\text{g, max}}, P_{\text{t}}^{\text{total}}) & \text{if } P_{\text{t}}^{\text{total}} > 0 \\ 0 & \text{if } P_{\text{t}}^{\text{total}} \leq 0 \end{cases} \tag{10}$$

$$P_{\text{t}}^{\text{unmet}} = P_{\text{t}}^{\text{total}} - P_{\text{t}}^{\text{g2s}} \tag{11}$$

In Equation (1)–(11), the symbols represent:

SoC_t^{b}: SoC of the BESS at time t (%).

P_t^{b}: Power of the BESS at time t (W).

$E^{\text{b, r}}$: Rated energy capacity of the BESS (Wh).

P_t^{g2s}: Power supplied from the grid to the station at time t (W).

P_{c}^{r}: Rated power of the charger c (W).

P_t^{s2ev}: Total power supplied from the station to HDEVs at time t (W).

P_t^{s2g}: Power supplied from the station to the grid at time t (W).

P_t^{unmet}: Unmet power demand at time t (W).

P_t^{pv}: Power generated by the PV panels at time t (W).

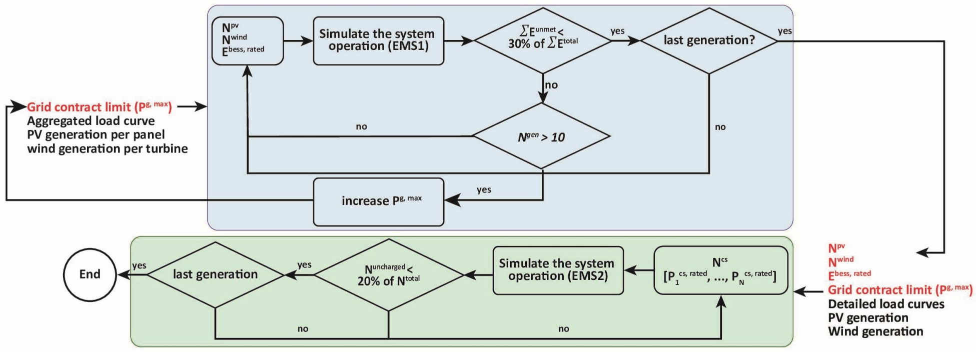

Fig. 1: General block diagram of the sizing model.

P_t^{wind}: Power generated by the wind turbines at time t (W). P_t^{wind}

$P_{\text{t,v}}^{\text{ev}}$: Power demand of vehicle v arriving to the station at time t (W).

N^{ev}: the total number of HDEVs arriving at the station at time t.

As shown in Fig. 1, the sizing model operates across two distinct optimization levels. At the first optimization level, a holistic view of the system is taken, focusing on optimizing the sizes of the BESS ($E^{\text{b, r}}$) and RESs, including the number of PV panels (N^{pv}) and wind turbines (N^{wind}). In this layer of the model, the objective is to identify the optimal system configuration that fulfills most of the energy demand for HDEV charging ($E_{\text{t}}^{\text{s2ev}}$) while minimizing the electricity purchase expenditure over the simulation period (T), penalties for unmet demand ($E_{\text{t}}^{\text{unmet}}$) based on the grid limit ($P^{\text{g, max}}$), and the NPV of investment cost (I_1). Prioritization is given to minimizing the unmet demand energy in this layer. In the final selection process, any points on the pareto front where the unmet demand exceeds 30% of the total charging demand (E^{total}) are disregarded, as shown in Fig. 1. Subsequently, the optimal combination is selected from the remaining pareto front points based on the fitness function presented in (12). In the first layer of the model, a dynamic adjustment procedure is started if the defined grid limit ($P^{\text{g, max}}$) is insufficient to meet the system's basic needs, and an appropriate configuration cannot be found under those requirements. This involves beginning the model with the updated grid limit and updated set of constraints. This iterative approach ensures that the charging station configuration aligns closely with both the operational demands of HDEVs and the constraints of the existing grid infrastructure.

$$Minimize(\alpha_1 \sum_{t=1}^{T} E_{\text{t}}^{\text{g2s}} \cdot c_{\text{t}}^{\text{g2s}} + \alpha_2 \sum_{t=1}^{T} E_{\text{t}}^{\text{unmet}} \cdot c_{\text{t}}^{\text{unmet}} + \alpha_3 \frac{I_1 \cdot T}{L}) \tag{12}$$

where:

$$I_1 = N^{\text{pv}} \cdot P^{\text{pv, r}} \cdot c^{\text{pv}} + N^{\text{wind}} \cdot c^{\text{wind}} + E^{\text{b, r}} \cdot c^{\text{b}} \tag{13}$$

In Equations (12) and (13), the symbols represent:

$c_{\text{t}}^{\text{g2s}}$: Cost of energy purchased from the grid at time t (€).

$c_{\text{t}}^{\text{unmet}}$: Penalty cost for unmet demand at time t (€).

L: Lifespan of the assets.

$P^{\text{pv, r}}$: Rated power of each PV panel (W).

c^{pv}: Cost of PV panel installation (€per rated power).

c^{wind}: Cost of wind turbine installation (€per wind turbine).

c^{b}: Cost of BESS installation (€per Wh).

After completing this first layer of optimization, the second layer is initiated. In the second level, a more detailed perspective is adopted, considering individual components within the system. Here, the objective is to determine the number of chargers (N^{cs}) and rated power ($P^{\text{cs, r}}$) of each charging plug in the station, ensuring efficient utilization of resources and effective meeting of the operational demands of HDEVs. The objective is to optimize this configuration to efficiently charge HDEVs while minimizing the penalties for unsatisfied charging demand and idle chargers (C^{idle}) (17) beside the NPV for purchasing and installing chargers (I_2) (16). In this stage, priority is given to minimizing unsatisfied charging demand. During the final selection process, any points on the pareto front where the number of trucks leaving the charging station without being charged ($N^{\text{uncharged}}$) exceeds 20% of the total number of trucks (N^{total}) are disregarded. Subsequently, the optimal combination is selected from the remaining pareto front points based on the fitness function presented in (14).

$$\min(\beta_1 \sum_{t=1}^{T} E_{\text{t,v}}^{\text{unmet}} \cdot c_{\text{t}}^{\text{unmet}} + \beta_2 C^{\text{idle}} + \beta_3 \frac{I_2 \cdot T}{L}) \tag{14}$$

where:

$$E_{\text{t}}^{\text{unmet}} = \begin{cases} \sum_{v=1}^{N^{ev}} \frac{(SoC_v^{\text{req}} - SoC_{\text{t, v}}) \times E_v}{100} & \text{if } t = t_{\text{dep}} \\ 0 & \text{otherwise} \end{cases} \tag{15}$$

$$I_2 = \sum_{c=1}^{N^{cs}} P_c^{\text{cs, r}} \cdot c^{\text{cs}} \tag{16}$$

$$C^{\text{idle}} = \frac{\sum_{t=1}^{T} \sum_{c=1}^{N^{cs}} (1 - U_{\text{t,c}})}{L} \cdot I_2 \tag{17}$$

In Equations (14)–(17), the symbols represent:

c_{cs}: Cost of high power charger installation (€/kW).

$U_{\text{t,c}}$: A binary variable indicating whether each charger is working or not utilized at time t.

The system operation in both layers is simulated using a rule-based energy management (EMS). The primary rationale behind using a rule-based EMS is to prioritize simplicity and efficiency. Given the necessity to execute this algorithm many times for each generation of the GA (once every 15 minutes for the simulation period), it is crucial to maintain a swift

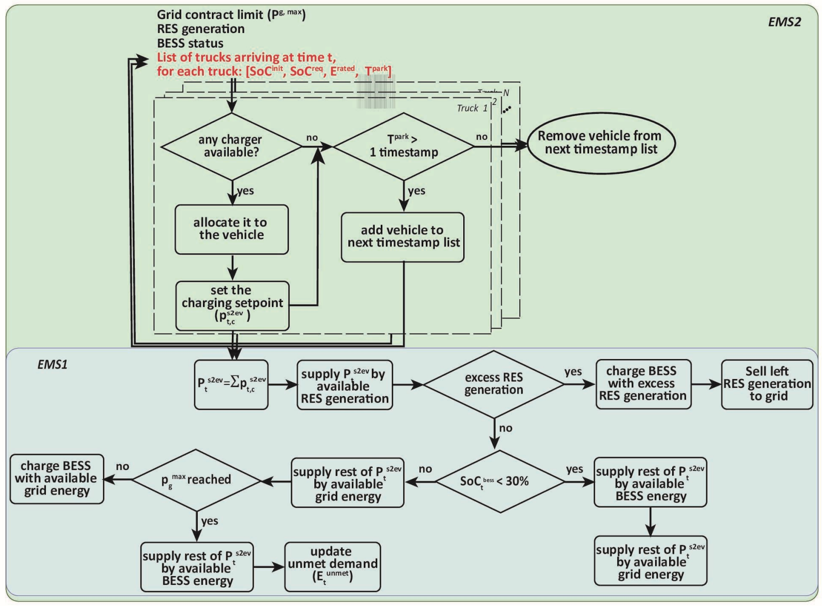

Fig. 2: General block diagram of the rule-based EMS deployed in the sizing model.

and straightforward approach. Fig. 2 presents the general block diagram of the rule-based EMS deployed in the sizing model.

Since the focus is on identifying the general or high-level architecture of the system in the first layer, the total charging demand (P_t^{s2ev}) is considered, and only the blue section of this block diagram is utilized (EMS1). However, in the second layer of the sizing model, which is responsible for determining the chargers' rated power, the detailed charging demand ($T_{\text{t,v}}^{\text{park}}$, $SoC_{\text{v}}^{\text{ev, init}}$, $SoC_{\text{v}}^{\text{ev, req}}$, $E_{\text{v}}^{\text{ev, r}}$) is considered instead of the aggregated load curve, and the charger allocation block is activated as well (EMS2 in Fig. 2). At each timestamp, several HDEVs arrive at the charging station to be charged. The EMS first checks if there are any available chargers. If a charger is available, the first arrived vehicle connects to the charger, and the charging process starts. However, vehicles where no charger is available need to wait until the next timestamp. The parking time (T^{park}) for each vehicle is assumed to be known, so if no charger is allocated to the vehicle before its parking time ends, the vehicle leaves the station without being charged, incurring a penalty. Additionally, since there is a possibility that chargers may not be allocated in time, some vehicles may leave the station without being fully charged. When the total charging demand is calculated, the source allocation is initiated. The EMS is designed to prioritize utilizing available RES generation to meet the energy demand at each timestamp. If the demand exceeds the available RES generation, the BESS is utilized, followed by the grid as a last resort. This approach aims to reduce dependence on the grid and promote self-sufficiency. The BESS is charged whenever its SoC falls below 30%, and the grid has available capacity.

III. Case Study

Solar and wind generation data for modeling is sourced from [9]. Additionally, the data related to charging demand, including the arrival times of trucks at the charging station, their battery capacity, and energy demand upon arrival, is obtained from the

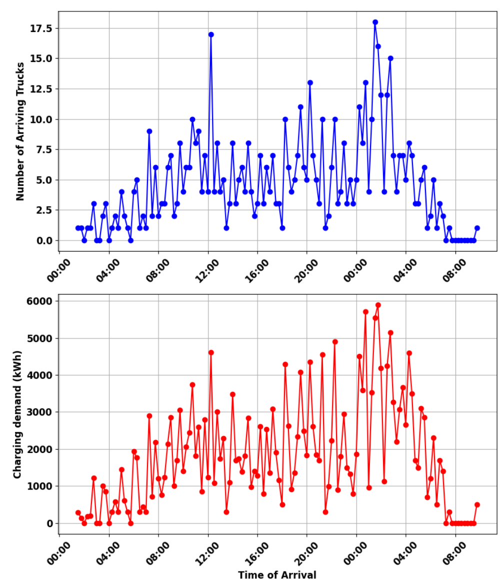

Fig. 3: Charging demand at an HDEV charging station under study.

outputs of a truck trip simulator called MASSGT [10]. The simulator models truck movements within the Netherlands based on real trucks' and trailers' GPS data. Using this data, a semi-realistic charging demand dataset for eight HDEV charging stations within the Netherlands is generated. Fig. 3 illustrates the dataset related to one of the chosen charging stations used in the sizing model. The data related to the price of electricity purchased from the grid is obtained from the Ember website, which sources its data from Entso [11]. The price of electricity purchased and sold to the grid is considered to be the same. Additionally, the cost of charging HDEVs at the charging station is assumed to be 0.6 €/kWh according to [12]. To account for seasonal changes in RES generation and electricity costs, the final dataset includes data from the first week of each season from the entire dataset. Besides, in all the equations above, the penalty for unsatisfied charging demand is set to three times the electricity purchase price at that time.

The range of decision variables in the sizing model plus their costs are shown in Table I. It should be noted that the choices of BESS rated power and chargers' rated power, shown in this table, are step-wise. This is because these elements are constructed using modules, mirroring real-world scenarios. The ratings can be adjusted in increments of 100 kWh for the BESS and 100 kW for the chargers' rated power. Moreover, the lifetime of all assets, including PV panels, wind turbines, BESS, and chargers, is considered 20 years.

TABLE I: Optimization variables used in the sizing model.

Variable	Lower limit	Upper limit	Unit size	investment cost
N_{pv}	0	2770	365 W	365 €/panel
N_{wind}	0	5	3.5 MW	6125000 €/turbine
N_{cs}	1	15	–	–
$P^{\mathrm{r}}_{\mathrm{cs}}$	300 kW	1 MW	100 kW	500 €/kW
E^{r}_{b}	100 kWh	2 MWh	100 kWh	290 €/kW

IV. Results

In the following, results using the above-described sizing model are shown. In Fig. 4a, the dynamic evolution of decision variables within the first layer GA is depicted, offering a comprehensive insight into the iterative progression of initial fronts across generations. The simulation commenced with a grid contract limit of 3 MW. However, as this limit failed to meet the model's set constraints and requirements, it was gradually increased to 4.5 MW. The results presented in this section are for a system configuration with a grid limit set to this increased value. Notably, it can be observed that each pareto front encompasses more than a single combination, showcasing the diverse range of potential solutions capable of achieving optimal system configuration. This diversity is particularly pronounced in the NSGA-II algorithm, where each objective is minimized independently, yielding a spectrum of non-dominated solutions. Upon analysis of these results, it becomes evident that the optimal configuration, tailored to meet the specifications and operational constraints of the system, entails the deployment of 37 PV units, 0 wind turbines, alongside a BESS boasting a capacity of 2 MWh. The corresponding values for different objectives considering this configuration are as follows: NPV of investment cost of 2276.46 €, total electricity cost of 68.49 k€, and unmet demand penalty of 70.91 k€. With this configuration, the percentage of unmet demand is 27.1%. Upon completion of the first layer of optimization, the final system configuration is transferred to the second layer, tasked with determining the number of charging stations and their power ratings. Fig. 4b illustrates the dynamic evolution of decision variables within the second layer GA. Similar to the first layer, each pareto front encompasses multiple combinations, demonstrating the diverse array of potential solutions capable of achieving an optimal system configuration. Upon analyzing these results, the optimal

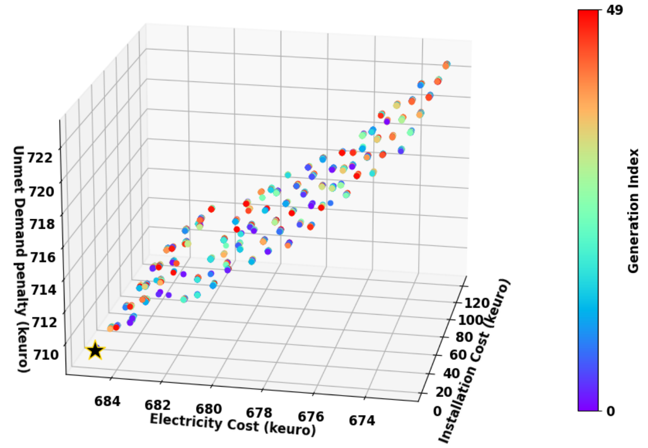

(a)

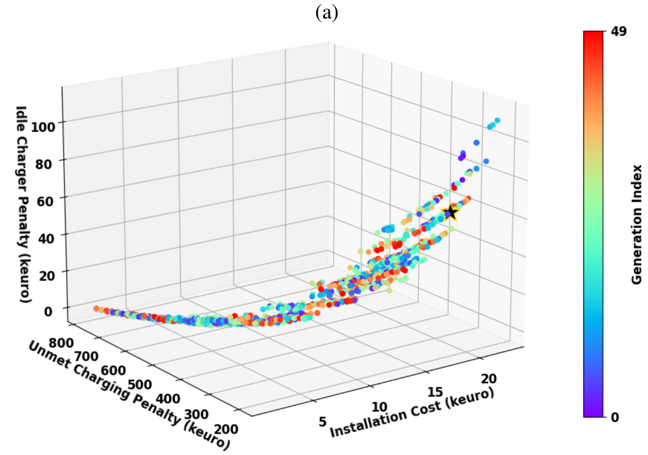

(b)

Fig. 4: Evolution of pareto fronts at each iteration within the (a) first layer and (b) second layer of the optimization model.

configuration which meets system specifications and operational constraints involves deploying 13 chargers with power ratings of [500, 500, 600, 600, 600, 700, 700, 800, 800, 900, 900, 1000, 1000] kW. Correspondingly, considering this configuration, the associated values for different objectives are as follows: NPV of investment cost of chargers at 18.41 k€, unmet charging penalty at 20.51 k€, and idle charger penalty at 67.59 k€. Additionally, with these asset sizes, 48.4% of vehicles are fully charged, 33.9% are undercharged, and the remaining 17.7% leave the charging station without being charged. In the identified system configuration, wind turbines were not included, likely due to their high rated power per unit and investment cost compared to PV and BESS. This makes them less practical for this charging station's requirements. Additionally, since the simulation was conducted using data specific to the Netherlands, where solar irradiance is not so high throughout the year, the number of PV panels was not selected to be high either. Figure 5 illustrates how the percentage of uncharged, undercharged, and fully-charged trucks changes with the number of PV panels in the system. It is evident from the case study that increasing the number of PV panels does not have a significant impact, and the optimization model opted for the lowest value to minimize investment costs.

Fig. 6 presents the results obtained from simulating the

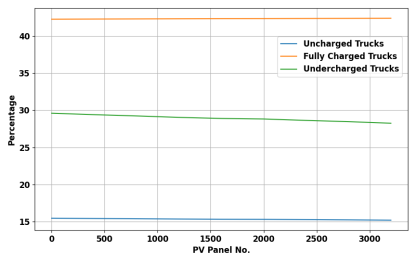

Fig. 5: Effect of PV panel quantity on truck charging status.

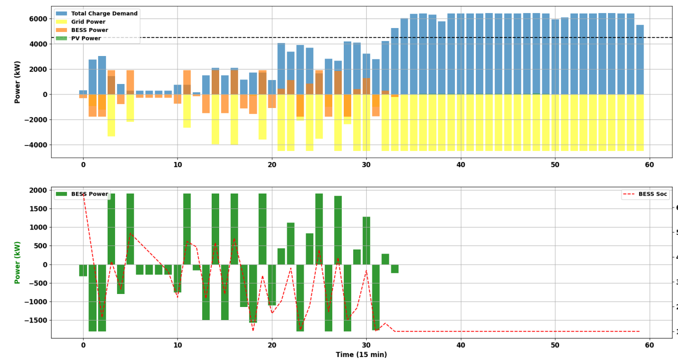

Fig. 6: Upper plot: Power flow across primary subsystems of the charging station. Lower plot: Detailed view of BESS energy and SoC throughout the simulation period.

system performance using the rule-based EMS within the second layer, utilizing asset sizes determined during the optimization phase. In Fig. 6, the upper plot delineates the overall power flow across primary subsystems of the EH over the course of a period of 3,5 hours. Meanwhile, the lower plot offers a detailed perspective on the BESS energy and SoC throughout the simulation period. Given the BESS's primary role as an energy source before grid utilization, frequent charge and discharge cycles are observed. At this simulation level, individual load curves for each charging station are considered, although for clarity and ease of interpretation, Fig. 6 showcases the aggregated charging demands. As observed, despite the inclusion of a large BESS in the system configuration, there is insufficient energy available during peak hours to assist in meeting the charging demand which highlights the importance of EMS in optimizing system operation.

V. Conclusion

This paper presents a bi-level multiobjective sizing model designed to address the critical need for optimized charging station configurations tailored specifically for HDEVs. By integrating various factors such as investment costs, penalties for unmet demand, idle chargers, rejection of HDEVs, and expenditure management, the model aims to strike a balance that maximizes economic and social benefits while meeting operational requirements. The model's outcomes provide valuable insights into the optimal sizing of assets within charging stations, including the number of PV panels and wind turbines, the capacity of BESS, grid connection capacity, and the configuration of chargers.

By examining the outcomes presented in section IV, the pivotal role of EMS in enhancing system performance becomes evident. Despite the presence of a quite big BESS within the system architecture, its effectiveness in meeting demand, particularly during peak hours, is hindered by the absence of smart charging mechanisms. Furthermore, the prioritization of objectives in multiobjective GA optimization and the final selection process of determining the optimal configuration from the pareto front significantly influence the system's configuration. As a result, future efforts will focus on enhancing the sizing model to incorporate smart charging mechanisms and assessing its efficacy under diverse operational conditions and selection modes.

Acknowledgment

This work was partially supported by the Dutch Ministry of Economic Affairs and Climate Policy under the project "Plug-in." The authors thank Manfredo Sartori for his efforts in building the charging demand curve at the HDEV charging station.

References

[1] IEA, *Global CO_2 emissions from transport by subsector, 2000-2030, IEA, Paris*, Available online: https://www.iea.org/data-and-statistics/charts/global-co2-emissions-from-transport-by-subsector-2000-2030, Accessed: 09/06/2023, 2021.

[2] The European Commission, *Green Deal: Greening freight for more economic gain with less environmental impact*, Available online: https://ec.europa.eu/commission/presscorner/detail/en/IP_23_3767, Accessed: 24/07/2023, 2023.

[3] The European Commission, *A European Green Deal*, Available online: https://commission.europa.eu/strategy-and-policy/priorities-2019-2024/european-green-deal_en, Accessed: 09/06/2023, 2020.

[4] The European Commission, *Regulation of the European Parliament and of the Council on the deployment of alternative fuels infrastructure, and repealing Directive 2014/94/EU of the European Parliament and of the Council*, Available online: https://eur-lex.europa.eu/legal-content/EN/TXT/?uri=CELEX\%3A52021PC0559, Accessed: 15/06/2023, 2021.

[5] Thomas S. Bryden, George Hilton, Borislav Dimitrov, Carlos Ponce de León, and Andrew Cruden, "Rating a Stationary Energy Storage System Within a Fast Electric Vehicle Charging Station Considering User Waiting Times," *IEEE Transactions on Transportation Electrification*, vol. 5, no. 4, pp. 879-889, 2019, doi: 10.1109/TTE.2019.2910401.

[6] Qiang Yang, Siyang Sun, Shuiguang Deng, Qinglin Zhao, and MengChu Zhou, "Optimal Sizing of PEV Fast Charging Stations With Markovian Demand Characterization," *IEEE Transactions on Smart Grid*, vol. 10, no. 4, pp. 4457-4466, 2019, doi: 10.1109/TSG.2018.2860783.

[7] J.A. Domínguez-Navarro, R. Dufo-López, J.M. Yusta-Loyo, J.S. Artal-Sevil, and J.L. Bernal-Agustín, "Design of an electric vehicle fast-charging station with integration of renewable energy and storage systems," *International Journal of Electrical Power & Energy Systems*, vol. 105, pp. 46-58, 2019, doi: 10.1016/j.ijepes.2018.08.001.

[8] Félix-Antoine Fortin, François-Michel De Rainville, Marc-André Gardner, Marc Parizeau, and Christian Gagné, "DEAP: Evolutionary Algorithms Made Easy," *Journal of Machine Learning Research*, vol. 13, pp. 2171-2175, 2012.

[9] Ibrahim Diab, Bram Scheurwater, Alice Saffirio, Gautham Ram Chandra-Mouli, and Pavol Bauer, "Placement and sizing of solar PV and Wind systems in trolleybus grids," *Journal of Cleaner Production*, vol. 352, pp. 131533, 2022, doi: https://doi.org/10.1016/j.jclepro.2022.131533..

[10] Michiel de Bok and Lóri Tavasszy, "An empirical agent-based simulation system for urban goods transport (MASS-GT)," *Procedia Computer Science*, vol. 130, pp. 126-133, 2018. doi: https://doi.org/10.1016/j.procs.2018.04.021.

[11] Ember, *European Wholesale Electricity Price Data*, Available online: https://ember-climate.org/data-catalogue/european-wholesale-electricity-price-data/, 2024.

[12] European Alternative Fuels Observatory, *Electric Vehicle Recharging Prices*, Available online: https://alternative-fuels-observatory.ec.europa.eu/consumer-portal/electric-vehicle-recharging-prices, 2024.